Radiology of colorectal cancer with emphasis on imaging of liver metastases

Pijl, M.E.J.

4

MR Imaging of Liver Metastases: Limitation of Spleen-Liver Model in Optimizing Pulse Sequences

Jeroen L. Turkenburg, Milan E.J. Pijl, Els L. van Persijn van Meerten,
Jo Hermans, Johan L. Bloem

JMRI 1999; 9:369-372

ABSTRACT

The spleen-liver model, as a predictor for contrast-to-noise ratio (CNR) in liver metastases, was verified for seven sequences in 22 patients with 70 colorectal metastases. Optimization of conventional spin-echo (SE), T1 magnetization-prepared gradient-echo and fat-frequency-selective presaturation inversion-recovery fast SE can be done using the spleen-liver model. CNR of liver-spleen and liver metastases, however, differed significantly ($P \leq .04$) on our T1 gradient-echo and T2-weighted fast SE images, with and without fat-selective saturation.

INTRODUCTION

Since spleen-liver contrast-to-noise ratio (CNR) was found to be similar to those of metastases-liver on conventional spin-echo (SE) sequences [1], the so-called spleen-liver model has been used in studies with healthy volunteers to optimize various T1-weighted sequences [2]. More recently, this model has also been used in newer more complicated pulse sequences [3-7]. Comparable spleen-liver and metastases-liver CNR were reported for T1 gradient-echo (GE) [1,4], T1 magnetization-prepared GE (MPGE) [4], and T2 fast SE [7], while conflicting data were presented for T1-GE [5], and T2 fast SE with and without fat suppression [4,6]. Nevertheless, the value of the spleen-liver model in optimizing these pulse sequences has never been evaluated statistically.

The purpose of our study was to test the use of the liver-spleen CNR as a predictor for metastases-liver CNR on various pulse sequences used in detecting hepatic metastases from colorectal carcinoma. Subsequent effects on detection or characterization of hepatic metastases were beyond the scope of our study.

MATERIALS AND METHODS

The medical ethical committee of our institution approved this protocol. We obtained informed consent from 22 consecutive patients, who were evaluated for suspected liver metastases from histologically confirmed colorectal carcinomas. The patient group consisted of six women and 16 men, who ranged in age from 37 to 76 years (mean 55 years). A total of 78 metastases was diagnosed on magnetic resonance (MR) images by a panel of two radiologists and was subsequently confirmed. Histological confirmation was obtained in at least one metastasis per patient and in 55 out of the total of 78 liver metastases (in four patients by percutaneous biopsy and in 18 patients during laparatomy for either liver resection or isolated liver perfusion). The diagnoses of the other 23 lesions were based on surgical palpation and combined image analyses of intra-operative ultrasound (US) and contrast-enhanced helical computed tomography (CT).

MR examinations were performed with a 1.5-T system (Gyroscan NT 15; Philips, Best, The Netherlands). In each patient seven pulse sequences were used (Table 1, Figure 1). Slices were 10 mm thick with an interslice gap of 1 mm, and the field-of-view measured 375 mm for all sequences, except for the T1-MPGE sequence. To improve signal-to-noise ratio for

Table 1. Parameters of Pulse Sequences.

Sequence	TR (ms)	TE (ms)	TI (ms)	Flip Angle	ETL	Matrix	NEX	Scan Time (minute)	Artifact Suppression Technique
T1-SE	600	15		90		205x256	2	6	FC, RC, PRESAT
T1-GE	50	9.2		60		128x256	2	2	BH, PRESAT
T1-MPGE	9.8	4.6	668	10		128x256	1	1	BH
T2-SE	2,000	45/90		90		205x256	2	8.2	FC, RC, PRESAT
T2 fast SE	dep.	120		90	16	205x256	4	6	FC, RT, PRESAT
SPIR fast SE	dep.	100		90	21	198x256	4	3	FC, RT, PRESAT
STIR fast SE	dep.	60	160	90	7	123x256	2	3.2	FC, RT, PRESAT

BH = breath-hold; dep.= dependent on respiratory frequency, average 2,000 msec (range, 1,700-2,400 msec); ETL = echo train length; FC = flow compensation; ms = msec = millisecond; NEX = number of excitations; PRESAT = superior and inferior axially oriented presaturation slabs; RC = respiratory compensation (reordered phase encoding); RT = respiratory-triggering; TE = echo time; TI = inversion time; TR = repetition time.

the T1-MPGE sequence [8], slice thickness was increased to 13 mm with an interslice gap of 1.3 mm, and the field-of-view was increased to 430 mm. The first echo (echo time 45 msec) of the T2-weighted SE was not used in the analysis. The fast SE sequences were performed both without and with short-tau inversion-recovery (STIR) and fat frequency spectral presaturation inversion-recovery (SPIR). Various artifact reduction techniques (Table 1) were used, including breath-hold in the T1-GE and T1-MPGE sequences. Flow compensation (gradient moment nulling) and superior and inferior axial oriented presaturation slabs were used in all non-breath-hold sequences. To prevent respiratory artifacts, respiratory compensation (phase reordering with reference to the respiratory cycle) was performed in the conventional T1-SE and T2-SE, while respiratory triggering was used in the fast SE sequences.

Signal intensity (SI) measurements were obtained from images using standard operator-defined regions of interest (ROI). The ROI for lesions was at least $1cm^2$. Eight metastases measured less than $1cm^2$ and were excluded from quantitative analysis. Analysis of these

small lesions was not reliable because of partial volume averaging. Finally, 70 metastases were evaluated in 22 patients. The ROI for measuring large liver metastases was placed in the periphery of the lesion, thus excluding necrotic areas. For each patient the mean value of SIs of the metastases was measured and used in the analysis.

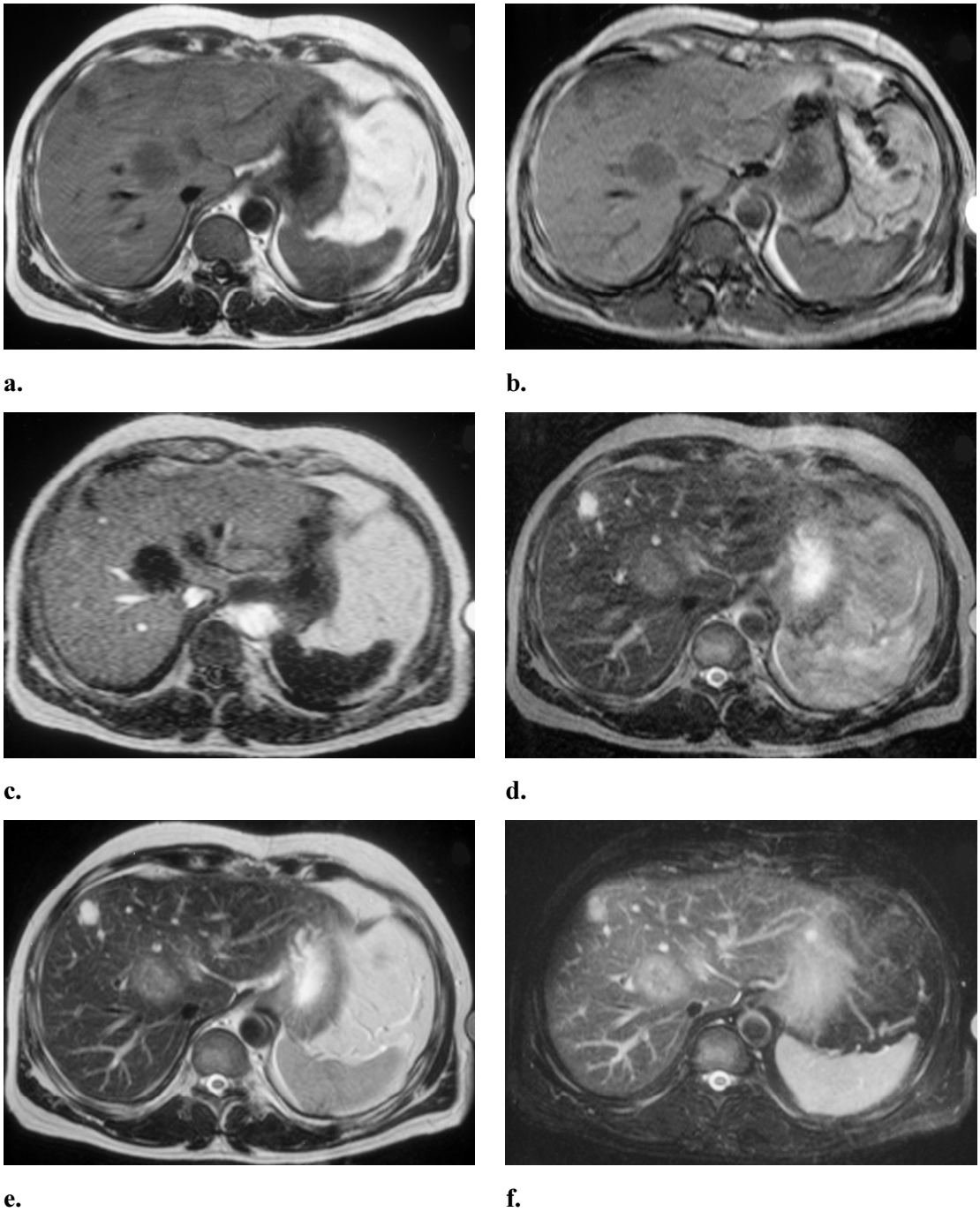

a. **b.** **c.** **d.** **e.** **f.**

Figure 1. Caption at next page.

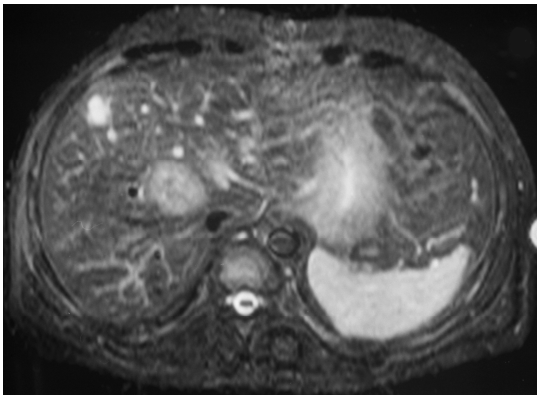

g.

Figure 1. Patient with two colorectal metastases centrally in the liver, a small cyst in segment II (not visible on all images, due to minor changes in image level), and a hemangioma ventrally in segment IV. (**a**) T1-SE image. (**b**) T1-GE image. (**c**) T1-MPGE image. (**d**) T2-SE image, second echo (echo time 90 msec). (**e**) T2 fast SE image. (**f**) Fat-frequency SPIR fast SE image. (**g**) STIR fast SE image.

The ROI for measuring liver parenchyma, spleen, and background noise were oval regions of 3cm^2, standardized for location. The ROI of the liver was located centrally in the right liver lobe, avoiding vessels as much as possible. The ROI of the spleen was taken in the center of the spleen. Background noise was measured in the phase-encoding direction, ventral to the patient, at the level of the center of the right liver lobe.

Contrast was quantified by the following formula: metastasis-liver CNR = (mean SI metastasis - SI liver parenchyma) / standard deviation of background noise; spleen-liver CNR = (SI spleen - SI liver parenchyma) / standard deviation of background noise [9].

Differences between spleen-liver CNR and mean metastases-liver CNR for each sequence were tested for statistical significance by means of the paired two-tailed Student *t* test. A *P* value of less than .05 was considered statistically significant.

RESULTS

The mean value and standard deviation of the spleen-liver CNR and metastases-liver CNR of the 22 patients are shown for each pulse sequence in Table 2. Compared with the metastases-liver CNR, the spleen-liver CNR was significantly lower ($P = .01$) on the T1-GE sequence and significantly higher on the T2 fast SE ($P = .04$) and SPIR fast SE ($P = .02$) sequences. On the T1-SE, T2-SE, T1-MPGE, and STIR fast SE sequences, spleen-liver CNR and metastases-liver CNR were not significantly different.

Table 2. Contrast-to-Noise Ratios

Sequence	CNR Spleen-Liver		CNR Metastases-Liver		*P* Value for Comparison of CNR
	Mean	SD	Mean	SD	Spleen-Liver versus Metastases-Liver
T1-SE	- 8.9	2.4	- 10.4	3.1	.11
T1-GE	- 7.3	2.3	- 9.3	2.1	.01[#]
T1-MPGE	- 12.3	2.1	- 12.4	3.1	.82
T2-SE	13.7	4.1	11.0	4.9	.12
T2 fast SE	35.0	8.2	28.4	12.4	.04[#]
SPIR fast SE	34.1	8.1	27.7	12.4	.02[#]
STIR fast SE	35.5	10.8	32.0	9.4	.20

Data are calculated mean ± SD CNR spleen-liver and CNR metastases-liver. Negative values indicate lower SIs for the spleen or metastases respectively, compared with the liver parenchyma. CNR = contrast-to-noise ratio; SD = standard deviation.
[#] *P* value < .05, indicating statistically significant difference.

Standard deviations of both metastases-liver and spleen-liver CNR were larger for T2-weighted sequences, compared with T1-weighted sequences. The high standard deviations of the metastases-liver CNR on the various T2-weighted fast SE sequences reflect the wide range of SIs of colorectal metastases.

DISCUSSION

Many research groups are improving the sensitivity of MR in the detection of hepatic metastases by implementing pulse sequences with improved CNR. The spleen-liver model is one of the instruments used in this endeavor. The spleen-liver model is based on the observation that liver metastases and spleen behave similarly with regard to SI on conventional SE sequences [1]. Like other authors [5], we confirmed similar spleen-liver and metastases-liver CNR on conventional T1-SE and T2-SE sequences. The spleen-metastases analogy can be used for optimization of these pulse sequences by quantitative analysis of SIs of liver parenchyma, spleen, and noise in healthy volunteers.

The spleen-liver model has also been used in newer more complex sequences at various field strengths [3-7]. Differences between spleen-liver and metastases-liver CNR have been reported for fat-suppressed T2 fast SE [6] and three-dimensional PSIF sequences, especially at large flip angles [3]. Spleen-liver CNR similar to metastases-liver CNR were reported for T1-

GE [1,4], T1-MPGE [4], and T2 fast SE [7]. However, conflicting data were presented for T1-GE [5] and T2 fast SE sequences [4,6]. The spleen-liver model correlated with liver-metastases CNR for T1 and T2 conventional SE, T1-MPGE, and STIR fast SE sequences. Significant differences were found between metastases-liver and spleen-liver CNR for T1-GE, T2 fast SE, and SPIR fast SE sequences (Table 2). Therefore spleen-liver CNR might not be the method of choice to optimize these sequences for the detection of hepatic metastases.

The contrast mechanism of some of the newer pulse sequences is rather complex and may account for differences between metastases and spleen. Relative to SE sequences, contrast in GE and fast SE sequences is also influenced by differences in relaxation time weighting, susceptibility, point spread function, stimulated echoes, diffusion, J-coupling, and magnetization transfer [10-12]. The fast SE sequences produce a larger diversity of SIs of metastases relative to spleen. Even in a group of colorectal metastases only, this is reflected by the high SD observed in the fast SE sequences with and without fat-selective saturation (Table 2). As shown by Siewert et al [4], the spleen-liver model becomes even less useful when the variety of lesions included in the analysis is extended to, for instance, several benign lesions.

The common occurrence of iron deposition in the reticuloendothelial system will affect the SI of the spleen. Although none of the patients in this study had a history of repeated blood transfusion or a disease like hemosiderosis, differences in iron load of the spleen could be reflected in the high SD observed in the various fast SE sequences.

A limitation of this study might be the choice of parameters of the T1-GE sequence. The rather long echo time of 9.2 msec is accompanied by T2* effects, but considering the flip angle of 60°, this GE sequence will predominantly have T1 contrast. An increase of repetition time and flip angle, combined with a shorter echo time, would probably have resulted in a higher CNR on T1-GE. Since each of these parameters influences image contrast separately, the final effect on CNR is almost impossible to predict. However, the results presented for T1-GE might be affected by the choice of parameters.

We conclude that the spleen-liver model can be used to optimize conventional SE, T1-MPGE, and STIR fast SE sequences. In this study, its value in predicting contrast between colorectal metastases and liver parenchyma on T1-GE, T2 fast SE, and SPIR fast SE sequences is limited. Since contrast mechanisms, especially in the newer and often more complex sequences, are subject to many parameters, applicability of the spleen-liver model has to be proved in each sequence again.

REFERENCES

1. Stark DD, Wittenberg J, Edelman RR, et al. Detection of hepatic metastases: analysis of pulse sequence performance in MR imaging. Radiology 1986; 159:365-370.
2. Semelka RC, Simm FC, Recht M, Deimling M, Lenz G, Laub GA. T1-weighted sequences for MR imaging of the liver: comparison of three techniques for single-breath, whole-volume acquisition at 1.0 and 1.5 T. Radiology 1991; 180:629-635.
3. Taupitz M, Speidel A, Hamm B, et al. T2-weighted breath-hold MR imaging of the liver at 1.5 T: results with a three-dimensional steady-state free precession sequence in 87 patients. Radiology 1995; 194:439-446.
4. Siewert B, Muller MF, Foley M, Wielopolski PA, Finn JP. Fast MR imaging of the liver: quantitative comparison of techniques. Radiology 1994; 193:37-42.
5. Saini S, Li W, Wallner B, Hahn PF, Edelman RR. MR imaging of liver metastases at 1.5 T: similar contrast discrimination with T1- and T2-weighted pulse sequences. Radiology 1991; 181:449-453.
6. Soyer P, Le Normand S, de Givry SC, Gueye C, Somveille E, Scherrer A. T2-weighted spin-echo MR imaging of the liver: breath-hold fast spin-echo versus non-breath-hold fast spin-echo images with and without fat suppression. AJR 1996; 166:593-597.
7. Kreft B, Layer G, Steudel A, et al. Evaluation of turbo spin echo sequences for MRI of focal liver lesions at 0.5 T. Eur Radiol 1994; 4:106-113.
8. de Lange EE, Mugler JP, Bosworth JE, et al. MR imaging of the liver: breath-hold T1-weighted MP-GRE compared with conventional T2-weighted SE imaging - lesion detection, localization, and characterization. Radiology 1994; 190:727-736.
9. Hendrick RE. Measurement of signal, noise, and SNR in MR Images. In: Hendrick RE, Russ PD, Simon JH, eds. MRI: principles and artifacts. 1st ed. New York: Raven Press Ltd., 1993; 2-6.
10. Outwater EK, Mitchell DG, Vinitski S. Abdominal MR imaging: evaluation of a fast spin-echo sequence. Radiology 1994; 190:425-429.
11. Constable RT, Anderson AW, Zhong J, Gore JC. Factors influencing contrast in fast spin-echo MR imaging. Magn Reson Imaging 1992; 10:497-511.
12. Henkelman RM, Hardy PA, Bishop JE, Poon CS, Plewes DB. Why fat is bright in RARE and fast spin-echo imaging. J Magn Reson Imaging 1992; 2:533-540.